Far-Infrared Absorption Spectra of Thick Superconducting Films*†

SCOTT L. NORMAN‡
Department of Physics and the James Franck Institute,§ University of Chicago, Chicago, Illinois
(Received 2 October 1967)

We have examined the absorption spectra of thick evaporated films of Pb, Sn, In, V, Ta, and Nb in the superconductive energy-gap region by a calorimetric detection technique. The intensity available from our far-infrared monochromator, together with the improved sensitivity of the detection system, made it possible to employ modulation techniques to obtain the derivatives of the absorption spectra of our samples. Multiple energy gaps were found for a Sn film and two thick Pb films, while a thinner Pb film and the other samples had single gaps. We suggest that these are the first far-infrared measurements to reveal multiple absorption edges in films. The energy gaps found for the two thick Pb films were $(4.18\pm0.04)kT_c$ and $(4.46\pm0.04)kT_c$ for one, and $(4.28\pm0.04)kT_c$ and $(4.65\pm0.04)kT_c$ for the other. For the Sn film, the gaps were $(3.58\pm0.02)kT_c$ and $(3.86\pm0.04)kT_c$. The gaps found for the other samples, in units of kT_c, were: for the thin Pb film, 4.34 ± 0.02; for In, 3.69 ± 0.04; for V, 3.4 ± 0.1; for Ta, 3.5 ± 0.2; and for Nb, 3.6 ± 0.2. These values are more precise than the earlier far-infrared results; in addition, the anomalously low values of $\sim 3kT_c$ obtained in previous far-infrared experiments for the Ta and Nb gaps are not reproduced in this work. The observed absorption edges are steeper than those predicted by either the extreme local or extreme anomalous limits of skin-effect theory. The energy gap of a thick Pb sample was measured as a function of magnetic field, this being the first such measurement by far-infrared calorimetric techniques. The gap was found to decrease by approximately 7% in going from zero field to the critical field for the bulk material (H_{cb}), in fair agreement with the Ginzburg-Landau theory. No gap was observed above H_{cb}, in agreement with previous observations on the superconducting surface sheath.

I. INTRODUCTION

THE observation of a threshold in the far-infrared or submillimeter absorption spectrum of a superconductor provides a direct measurement of the energy gap[1] in the single-particle excitation spectrum of that metal; the threshold energy $\hbar\omega_g$ is equal to $2\Delta(T)$, the value of the energy gap at the temperature of the measurement. Furthermore, the shape of the absorption spectrum of a metal gives a direct measurement of the variation with energy of the surface resistance, and it is of interest to compare these results with the predictions of the microscopic theory of superconductivity.[2] The directness of the interpretation of such spectroscopic data has resulted in several series of experiments concerned with the electromagnetic properties of superconductors, both as thin films[3–5] and in the bulk.[6–10] In the thin film work, the parameters measured were either the transmission[3,4] alone or the transmission and reflection.[5] It is possible to deduce from the transmission data the forms of the real and imaginary parts of the complex conductivity of the superconductor by invoking the Kramers-Kronig relations[3] connecting the two, as well as a conductivity sum rule.[11] The previous far-infrared work on bulk superconductors[6–8] consisted of measuring the change in the surface resistance of a metal which took place when superconductivity was destroyed by a magnetic field; a nonresonant cavity cast from the metal under investigation was illuminated by a far-infrared beam, and the radiation escaping from the cavity was measured. In this fashion, films of Pb, Sn, In, and Hg, and bulk samples of Pb, Sn, In, Hg, Ta, V, Nb, La, and Pb:Bi, Pb:Tl, and Pb:Sn alloys have been investigated. Calorimetric measurements, i.e., measurements of the heating of the sample upon the absorption of radiation, have been performed on Al[9] and Zn,[10] the energy gap values of which permit the use of millimeter- or even centimeter-wavelength radiation generated at relatively high power levels in conventional microwave circuits.

The work which we report here was undertaken in order to measure any structure present on the absorption edges of superconductors having energy gaps of the order of 1 meV; these are the metals for which far-infrared techniques must be employed. In contrast to the earlier workers who used such techniques, however, we chose to make direct calorimetric measurements because of the simplicity of their interpretation. Because the power levels involved are quite low (typically, 10^{-8}–10^{-9} W of radiation incident on the sample), it is necessary to employ very small samples and very

* Supported in part by the U.S. Army Research Office (Durham) and the Advanced Research Projects Agency.
† Submitted in partial fulfillment of the requirements for the Ph.D. degree at the University of Chicago.
‡ Present address: Automatic Electric Laboratories, Northlake, Ill. 60164.
§ Formerly the Institute for the Study of Metals.
[1] J. Bardeen, L. N. Cooper, and J. R. Schrieffer, Phys. Rev. **108**, 1175 (1957).
[2] D. C. Mattis and J. Bardeen, Phys. Rev. **111**, 412 (1958).
[3] R. E. Glover, III, and M. Tinkham, Phys. Rev. **108**, 243 (1957).
[4] D. M. Ginsberg and M. Tinkham, Phys. Rev. **118**, 990 (1960).
[5] L. H. Palmer, Ph.D. thesis, University of California, 1966 (unpublished); L. H. Palmer and M. Tinkham, Phys. Rev. (to be published).
[6] P. L. Richards and M. Tinkham, Phys. Rev. **119**, 575 (1960).
[7] J. D. Leslie and D. M. Ginsberg, Phys. Rev. **113**, A362 (1964).
[8] J. D. Leslie, *et al.*, Phys. Rev. **134**, A309 (1964).
[9] M. A. Biondi and M. P. Garfunkel, Phys. Rev. **116**, 853 (1959).
[10] S. A. Zemon and H. A. Boorse, Phys. Rev. **146**, 309 (1966).
[11] R. A. Ferrell and R. E. Glover, III, Phys. Rev. **109**, 1398 (1958); M. Tinkham and R. A. Ferrell, Phys. Rev. Letters **2**, 331 (1959).

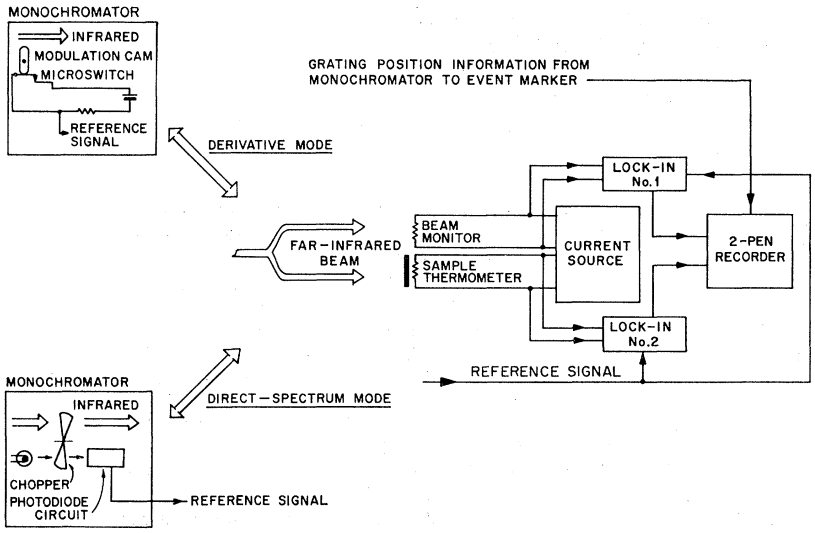

FIG. 1. Schematic of experiment.

sensitive thermometric techniques in such an investigation. Our early work[12] involved the use of Pb foils 0.005 cm thick as samples; subsequent work, however, has been performed with vacuum-deposited "thick" films of Pb, Sn, In, Nb, V, and Ta. By using mica substrates approximately 0.002 cm thick, we have achieved significant reductions in the thermal mass of our samples. It should be reiterated that in all cases our sample thicknesses are many times the electromagnetic penetration depth; i.e., a thermometer attached to the rear of the substrate will not "see" any radiation being transmitted through the sample, but will respond only when the sample absorbs radiation with subsequent heating.

Our experiments, then, extend the use of the direct calorimetric technique to several metals not previously investigated in this manner. In addition, our optical instrumentation reflects some of the advances made in far-infrared technology since the earlier investigations. The superior energy resolution of our monochromator and the improved detector sensitivity which we have been able to achieve have made it possible to extract considerably more information from the absorption spectra than has been previously available. In particular, we have been able to obtain evidence for the existence of multiple energy gaps in several of our samples; the anisotropy of the superconducting energy gap in k space has been previously demonstrated in tunneling and ultrasonic attenuation experiments[13] and in one far-infrared investigation of single-crystal Sn.[14] Our results are in generally good agreement with those obtained from earlier tunneling experiments. This is true even of our Ta and Nb samples, whereas the earlier bulk-absorption measurements[6] resulted in anomalously low values of the energy gaps in these metals. It would appear that the previous results were influenced by the presence of gases dissolved in the surface layers of the samples. An interesting observation made in the course of our investigations was the apparent instrumental origin[15] of the precursor absorption,[12] an apparent absorption in Pb of radiation of quantum energy less than the gap value, which had also been reported by previous investigators.[4,6]

II. EXPERIMENTAL APPARATUS AND PROCEDURES

The experimental arrangement is shown schematically in Fig. 1. A grating monochromator was used to generate far-infrared radiation, which was transmitted to the sample by tapered metal light pipes. The sample film was suspended below a pumped He^4 bath, and a thermometer resistor cemented to the rear of the substrate detected the temperature rise which accompanied the absorption of radiation. Because the output spectrum of the monochromator was, in general, a function of energy (especially near the blaze energies of the various gratings), it was necessary to use a second resistor as a bolometer to monitor the intensity of the incident beam. The low-signal levels involved necessitated the use of phase-sensitive detection techniques; the output signals of the two lock-in amplifiers, which were proportional to the powers absorbed in the sample and beam monitor, respectively, were recorded on a two-pen stripchart recorder. The ratio of the two signals provided a measure of A_S, the absorptivity of the superconducting sample; the sample was then driven normal by a magnetic field and the experiment repeated to determine the normal-state absorp-

[12] S. L. Norman and D. H. Douglass, Jr., Phys. Rev. Letters **17**, 875 (1966).

[13] For a review of the tunneling experiments, see G. I. Rochlin, Phys. Rev. **153**, 513 (1967). The ultrasonic attenuation results are summarized in Table III.

[14] P. L. Richards, Phys. Rev. Letters **7**, 412 (1961).

[15] S. L. Norman and D. H. Douglass, Jr., Phys. Rev. Letters **18**, 339 (1967).

tivity, A_N. Various absorptivities and ratios are presented in Sec. IV.

In addition to the mode of operation described above, in which the absorption spectrum was recorded directly, it was also possible to operate the monochromator so as to obtain the derivative of the sample absorptivity with respect to energy. This proved to be especially useful when examining the threshold region of the absorption spectrum for evidence of multiple energy gaps.

A. Grating Monochromator

In Fig. 2 we show the optical path of the monochromator. The radiation source is a General Electric UA-3 quartz-jacketted mercury arc lamp, an image of which is formed on the entrance slit by the parabolic mirror. This slit is approximately 100 mm high and 5 mm wide, in order to capture as large a fraction of the lamp's radiation as possible. The Czerny-Turner optical path[16] permits the use of such long slits without the attendant problem of chromatic aberration, provided that the slit jaws are suitably curved.[17] In our instrument, the entrance and exit slits are laid out along circular arcs of radius approximately 190 mm, centered on the vertical center line of the slit plane. The plane and spherical mirrors following the exit slit then form a reduced image at the mouth of the monochromator condenser cone,[18] which transmits the radiation to the outer window of the cryostat.

As is common with far-infrared grating instruments, the energy resolution of our monochromator was set by the width of the exit slit. To scan the diffracted image of a line source across this slit required that the main grating be rotated by 0.5°; this "resolution width" became the unit of measurement for setting the sweep speed of the grating drive. The equation for the wavelength present at the center of the exit slit of an instrument such as ours is[19]

$$\lambda = 2d\gamma \sin\alpha, \tag{1}$$

where d is the grating spacing, γ is a geometrical constant, and α is the angle through which the main grating has been rotated from the zero-order position. Differentiating, we obtain the energy resolution of the instrument;

$$|d\nu| = d\lambda/\lambda^2 = (\cos\alpha/2d\gamma \sin^2\alpha)\,d\alpha \ (\text{cm}^{-1}) \tag{2}$$

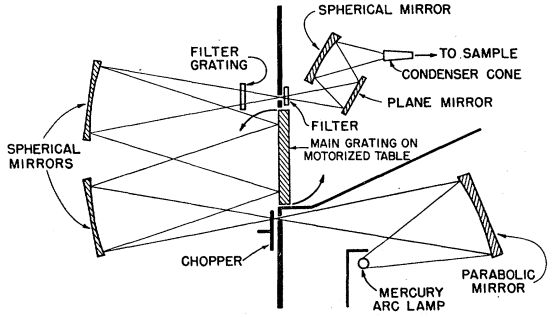

FIG. 2. Optical path of the F/2 Czerny-Turner monochromator.

TABLE I. Properties of diffraction gratings.

Grating Spacing, mm	Blaze energy, cm^{-1}	Useful range, cm^{-1}	Resolution, cm^{-1}	
			High-energy end	Low-energy end
0.76	25.1	17.1–40.9	2.1	0.34
0.89	21.5	14.7–35.1	1.8	0.29
1.13	16.9	11.6–27.7	1.4	0.23
1.40	13.6	9.3–22.3	1.1	0.18
1.90	10.0	6.8–16.4	0.8	0.14
2.26	6.8	5.8–13.8	0.7	0.11

The resolution obtainable from each of our main gratings at both ends of its useful range is tabulated in Table I, together with other properties of the gratings.

The main diffraction gratings were cut from stress-relieved aluminum blanks (Alcoa type 6061) approximately 305 mm square and 18 mm thick, using either a standard shaper or a milling machine, depending on the groove spacing desired. In general, it was found that the grooves cut on the shaper had the better finish. Six such gratings were made; although each provided a usable amount of radiation over an energy range of about 2.5:1, it proved desirable to overlap the regions covered in order that the various blaze energies might fall at points of particular interest in various spectra.

It is well known that the elimination of unwanted radiation is of the utmost importance in far-infrared experiments of this nature; in particular, we wish to use the radiation diffracted from the main grating in first order while rejecting that diffracted in higher orders. We accomplished the necessary selection by means of transmission filters at room temperature and within the cryostat. In particular, we used transmission gratings[20] to diffract the most troublesome radiation (that diffracted from the main grating in second and third order) out of the beam. This radiation then struck baffles within the monochromator, while the desired first-order radiation passed through the exit slit. Our transmission gratings were cast in Emerson and Cuming Stycast No. 1266 epoxy approximately 1 mm thick on aluminum forms which had been cut on a shaper. In contrast to the main echelette gratings, which had groove angles of 16° or 20°, these forms were cut with symmetrical 45° sawtooth grooves; in their investigation of the characteristics of such filter gratings, Moller and McKnight[20] reported that this groove shape

[16] The development of this optical system is reviewed in W. G. Fastie, J. Opt. Soc. Am. **42**, 641 (1952).
[17] W. G. Fastie, J. Opt. Soc. Am. **42**, 647 (1952).
[18] D. E. Williamson, J. Opt. Soc. Am. **42**, 712 (1952).
[19] See, e.g., J. E. Stewart and W. S. Gallaway, Appl. Opt. **1**, 421 (1962).
[20] K. D. Moller and R. V. McKnight, J. Opt. Soc. Am. **55**, 1075 (1965).

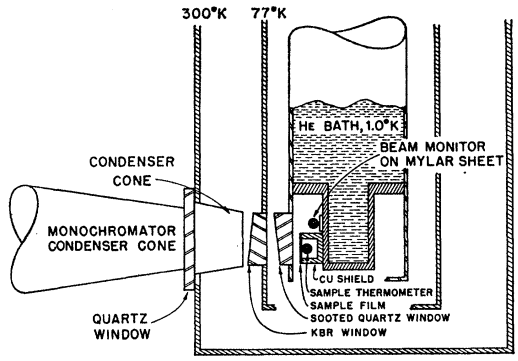

FIG. 3. Sample arrangement.

provided the best null in the transmission characteristics.

Additional filtering action at the cryostat was provided by sooted fused quartz windows at room temperature and approximately 1°K, and a KBr window at 77°K. The useful bandpass characteristics of this particular combination of cryogenic filters have been reported by Wheeler and Hill.[21] An additional filter of Teflon or black polyethylene was installed at the monochromator exit slit. The monochromator was housed in an evacuable aluminum case to permit the elimination of water-vapor absorption, although in practice the beam monitor allowed us to run the instrument with a dry N_2 flush or even with ambient atmosphere.

The amount of radiation provided by our monochromator, coupled with the sensitivity attained in our detection chain, enabled us to scan the absorption spectra of our samples continuously. The main grating table was driven by a variable-speed dc motor; typical scanning speeds used lay between 45- and 150-sec/resolution width. When the instrument was used in this mode, the radiation beam was chopped by a rotating blade located just inside the entrance slit. The blade was driven by a synchronous motor, and a variable-frequency oscillator allowed us to vary the chopping frequency to obtain the best response from the detectors. The frequencies used lay between 1.5 and 4.5 Hz. The chopper also interrupted a light beam which triggered a photodiode circuit, thereby providing reference drive for the lock-in amplifiers.

When examining the threshold regions of an absorption spectrum for structure (such as that expected to arise from multiple-energy gaps), it is useful to be able to differentiate that spectrum. It has been pointed out by Bonfiglioli *et al.*[22,23] that this can be readily done in a monochromator by imposing a periodic modulation on the photon energy appearing at the exit slit, and phase-sensitively detecting at the modulation frequency. The output of the lock-in amplifier fed by the sample thermometer, for example, is then proportional to

$$d[A(E)I(E)]/dE,$$

where $A(E)$ is the energy-dependent absorptivity of the sample, and $I(E)$ is the output spectrum of the monochromator. In our instrument, the modulation was accomplished by a motor-driven cam which caused the main grating to oscillate while the grating table was slowly swept through the region of interest. The cam was driven by a synchronous motor similar to that employed to drive the chopper described above. This chopper was not used when the monochromator was run in the derivative mode, reference drive for the lock-in amplifiers being supplied by a microswitch actuated by the modulation cam. Modulation frequencies between 1.5 and 4.5 Hz were employed. We found that the best compromise between signal-to-noise ratio and loss of detail in the spectrum was obtained when the modulation width was set to ± 1 resolution width; i.e., the cam caused the main grating to oscillate through $\pm 0.5°$ about its equilibrium position.

The output of the sample thermometer channel when the derivative mode was employed was proportional to

$$[dA(E)/dE]I(E)+A(E)[dI(E)/dE]$$

as explained above. If a grating was selected which had a relatively flat output spectrum in the region of interest, then any structure in the recorder trace for this channel could be attributed to structure in the absorption spectrum of the sample.

B. Detection Systems

In Fig. 3 we show the cryogenic radiation filters and the arrangement of the sample can. The cryostat was of conventional all-metal construction, and was mounted in close proximity to a 4-in. Stokes diffusion pump which was capable of pumping the He bath to approximately 0.995°K. At this point the beam monitor and sample thermometer would come to equilibrium at approximately 1.02°K. The bath temperature was regulated by means of an electronic bridge based on that described by Blake and Chase[24]; we found that with careful adjustment this bridge would hold the temperature constant to $\pm 5\mu$°K for periods of 20–30 min.

The beam monitor and sample thermometer were 1/10-W Allen-Bradley carbon resistors having room-temperature resistances of 150 Ω. At the temperature reached in most of the experimental runs, the resistances rose to approximately 1 MΩ, with logarithmic decrements of approximately $6°K^{-1}$. The beam monitor was cemented with General Electric 7031 varnish to a Mylar sheet which was in turn cemented to the Cu tailpiece of the cryostat. The sample thermometer was cemented to the back of the sample film's substrate;

[21] R. G. Wheeler and J. C. Hill, J. Opt. Am. **56**, 657 (1966).
[22] G. Bonfiglioli and P. Brovetto, Appl. Opt. **3**, 1417 (1964).
[23] G. Bonfiglioli *et al.*, Appl. Opt. **6**, 447 (1967).
[24] C. Blake and C. E. Chase, Rev. Sci. Instr. **34**, 984 (1963).

TABLE II. Sample properties.

Sample	Thickness, Å (±10%)	T_c(°K)	Resistance ratios Film	Bulk	Starting material source
Pb-I	6 000	7.15[a]	170	3500	Cominco "59" grade wire
Pb-II	10 000	7.15[a]	220	3500	Cominco "59" grade wire
Pb-III	1 200	7.15[a]	38	3500	Cominco "59" grade wire
Sn-I	3 500	3.73[a]	123	8150	Cominco "59" grade wire
In-I	9 000	3.40[a]	304	6900	Cominco "59" grade wire
V-I	2 500	5.00±0.05	5.7	14.4	MRC "Grade I" Ingot
Ta-I	7 500	4.40±0.05	~3	200	Materials Research Corp.[b]
Nb-I	2 500	9.0±0.1	6	150	Materials Research Corp.

[a] Bulk material values.
[b] The details of the preparation of this material may be found in R. Glosser, Phys. Rev. 156, 500 (1967).

this was then cemented around the edges to a Cu shield box which prevented any radiation from striking the thermometer directly. The dimensions of the shield box and beam monitor support were chosen to make the thermal time constants approximately equal to the reciprocal of a typical chopping (or modulation) frequency; in this way we maximized the fluctuating voltages appearing across the two resistors as they reponded to the monochromator beam.[25] The Manganin leads were thermally "grounded" to the He can several inches before reaching the various resistors, to eliminate spurious heat leaks. The current sources for the detectors consisted of mercury batteries in series with carbon potentiometers. For maximum sensitivity, each potentiometer was adjusted so that its resistance was approximately equal to that of the detector to which it was connected.

The signal from the sample thermometer was detected by a Princeton Applied Research model HR-8 phase-sensitive detector; the beam-monitor signal was first amplified by a Tektronix RM-122 preamplifier, and then detected by a Princeton Applied Research model JB-5 phase-sensitive detector. For most runs, the integration time constants of both channels were set to 10 sec. Under these conditions, the sensitivity of each detector channel was approximately 10^{-12} W at the lowest temperatures reached.

The magnetic field required to drive the samples normal was supplied by an iron-core magnet located outside the cryostat and powered by a filtered dc supply. A comparison of beam monitor traces taken with and without the magnetic field showed no evidence of magnetic-field-induced changes in the resistor's characteristics.

III. SAMPLE PREPARATION

All sample films were approximately 1×2 cm in size and were prepared in an ion-pumped high-vacuum evaporator[26] at pressures ranging from 2×10^{-8} to approximately 5×10^{-7} Torr. The Pb, Sn, and In samples were produced by evaporation from Joule-heated boat sources, while the V, Ta, and Nb required the use of an electron-beam gun. As mentioned previously, the substrates employed in these experiments were mica sheets approximately 0.002 cm thick; these substrates were allowed to "float" at ambient temperatures during the evaporations of Pb, Sn, and In, but were electrically heated for the evaporations of V, Ta, and Nb.

Two monitor films were prepared simultaneously with the samples. One, approximately 0.4×1.0 cm, was deposited on a mica substrate similar to that used for the samples, and was employed for residual resistance ratio measurements. The other was deposited on a standard 18 mm square microscope slide cover glass, and was used (after receiving a thin Ag overcoating) in a multiple-beam interferometer[27] for thickness determinations. In the latter stages of the experiment, we were also able to monitor the film thickness during deposition by means of a quartz crystal oscillator deposition monitor.[28]

In Table II, we present some of the characteristics of our samples. The residual resistance ratios (the ratios of resistances at room temperature to those at 4.2°K) are given for the bulk starting materials and for the monitor films. For those metals having transition temperatures above 4.2°K, a magnetic field was used to quench the superconductivity, with corrections being made for the effects of magnetoresistance. We were unable, however, to employ this technique with our Nb film, because the magnet available to us for resistance ratio measurements was incapable of reaching the upper critical field of this sample. Therefore, the film was removed from the He bath and the voltage first appearing across it as it warmed through the transition was recorded. The resistances were measured with standard four-terminal techniques, contact to the films being made through silver conducting paint[29] for Pb, Sn, and In, and through In-soldered constants for V, Ta, and Nb.

[25] For an analysis of bolometer response, see, e.g., V. L. Newhouse, *Applied Superconductivity* (John Wiley & Sons, Inc., New York, 1964), Chap. 8.
[26] Ultek Corporation Model TNB.
[27] S. Tolansky, *Multiple Beam Interferometry* (Oxford University Press, New York, 1948).
[28] Sloan Instruments Omni II.
[29] Type SC13 Flexible Silver Micropaint: Micro-Circuits Co., New Buffalo, Mich.

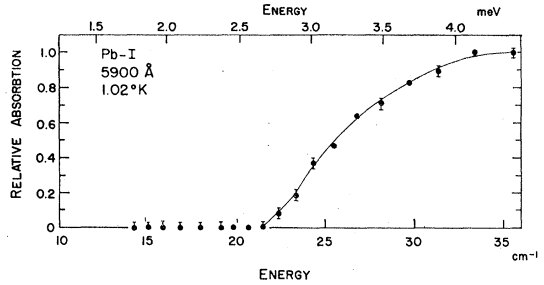

FIG. 4. Superconducting-state absorption in a Pb film sample.

Special care was taken to ensure that the transition temperatures of our V, Ta, and Nb samples approximated those of the bulk metals. It has been found,[30] for example, that a Nb film deposited at a pressure of 4×10^{-7} Torr had a transition temperature of only 5°K; this was presumably the result of contamination by residual oxygen. We were able to alleviate this problem by evaporating sufficient metal in our sample preparation system to obtain active gettering before the sample substrate was exposed, and by keeping the substrate at an elevated temperature during the evaporation. The techniques employed have been discussed by Neugebauer and Ekvall.[31]

Each sample was examined to ensure freedom from pinholes which could allow radiation to strike the thermometer resistor directly and thus give a false indication of absorption. The 150 Ω thermometer, which had been prepared by filing a flat surface on the resistance material, was then cemented to the rear of the substrate with a 50:50 mixture of General Electric 7031 and toluene.[32] The resistor leads were also thermally

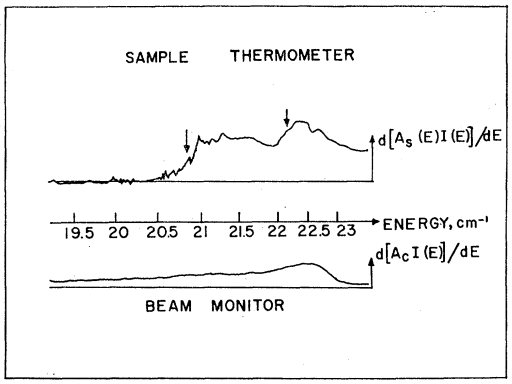

FIG. 5. Derivative-mode signals for the same sample as Fig. 4, illustrating the structure found in the gap region. A_c is the absorptivity of the carbon-resistor bolometer, which we assume to be independent of energy over this range. Scanned from high energies to low; arrows denote gap assignments.

tied to the substrate with this cement; this maximized the contact between thermometer and sample. Finally, the thermometer leads were attached and the substrate was cemented to the Cu shield box. It was found that this procedure could be carried out in approximately 30 min, which therefore constitutes the lower limit to the exposure of a sample to the atmosphere. It is not believed that any surface films formed in this length of time would be thick enough to distort the data through significant absorption of radiation; for example, the data of Morris and Tinkham[33] indicate that Sn and In probably form no significant oxide coating in so short a time, and that Pb forms only about 5 Å of oxide. In those cases in which the samples were not to be

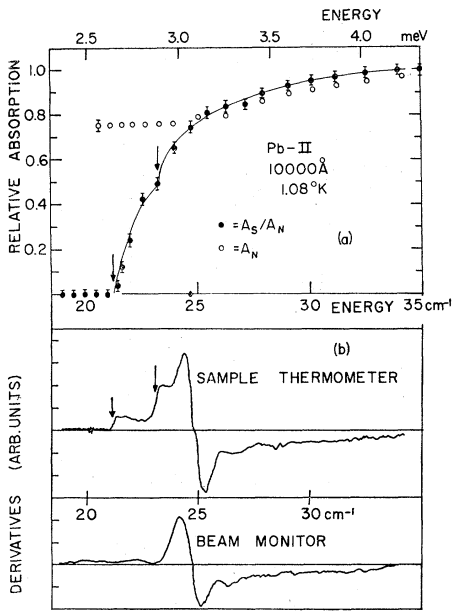

FIG. 6. (a) Normal-state absorptivity A_N and relative superconducting-state absorptivity A_S/A_N for a thick Pb film; (b) derivative-mode signals for this sample in the superconducting state. Arrows denote our gap assignments. The prominent feature appearing in both derivative traces is the derivative of the grating blaze peak.

mounted in the cryostat immediately after preparation, a vacuum dessicator was employed for storage.

IV. RESULTS

Our principal results, i.e., the absorption spectra and their derivatives for the various films, are presented in Figs. 4–12. While our raw data were continuous records of detector output voltages versus energy, the division of sample thermometer voltage by beam monitor voltage to give a relative absorption figure was carried out "by hand" at discrete energies, separated by approxi-

[30] D. H. Douglass, Jr. (private communication).

[31] C. A. Neugebauer and R. A. Ekvall, J. Appl. Phys. **35**, 547 (1964).

[32] Previous experimenters have also reported the use of similar thermometers cemented to a glass substrate prior to film deposition, with no apparent damage to the resistor during the evaporation. See T. Seidel and H. Meissner, Phys. Rev. **147**, 272 (1966).

[33] D. E. Morris and M. Tinkham, Phys. Rev. **134**, A1154 (1964).

mately one resolution width. We obtained in this fashion both superconducting and normal-state absorptivities A_S and A_N for samples Pb-II, Pb-III, Sn-I, and In–I. In Figs. 6(a), 7(a), 8(a), and 9(a) we present A_N (arbitrarily normalized) and A_S/A_N for these samples. Most of the error bars on the A_N data have been suppressed for clarity; these generally amounted to approximately 2%. In Fig. 5 and the lower portions of Figs. 6–9 we present the sample thermometer and beam monitor traces obtained with the monochromator running in the derivative mode and the sample superconducting. As discussed in Sec. II A, these traces represent the derivatives of the product of the monochromator output spectrum and the absorption spectrum of either the sample or the beam monitor. If we

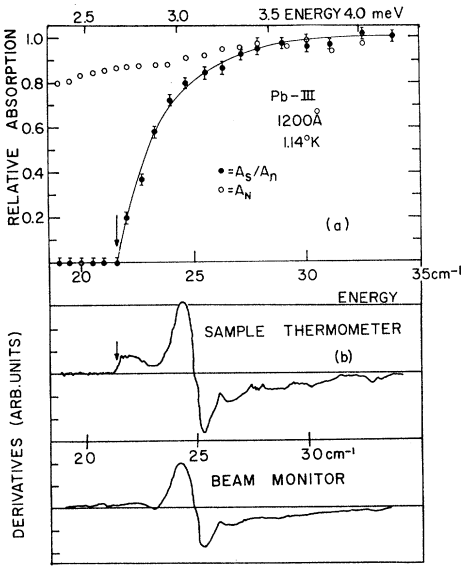

FIG. 7. (a) A_N and A_S/A_N for a thin Pb sample; (b) derivative signals. Note the appearance of only one gap.

assume that the latter has an energy-independent absorptivity over the restricted range of interest, then structure appearing in the traces can be assigned to either the monochromator spectrum or the sample's absorptivity spectrum. Structure appearing simultaneously in both traces is assumed to be characteristic of the monochromator (or possibly indicative of a bath-temperature fluctuation), while structure appearing only in the sample thermometer trace presumably belongs to the sample absorptivity characteristics. The vertical arrows indicate our assignments of gap values. The spectral scan was from the higher energies to the lower, and the broadening of the breaks in the sample thermometer derivative curves at the gap energies arises from instrumental effects such as the long integration times of the lock-in amplifiers. The very prominent feature appearing simultaneously in both members of a derivative-trace pair is the derivative of

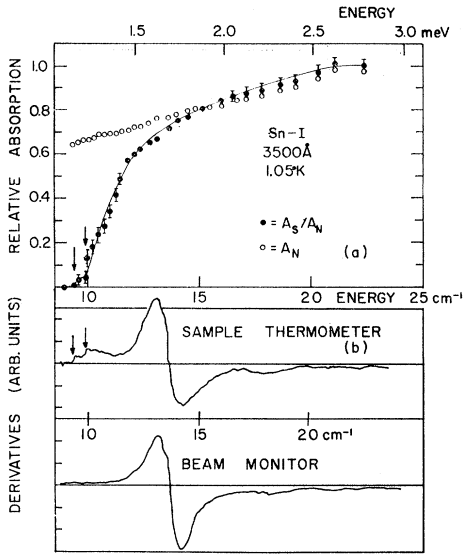

FIG. 8. (a) A_N and A_S/A_N for a Sn sample; (b) derivative signals.

the monochromator output spectrum near the blaze energy of the main grating.

For sample Pb-I, which was prepared before our magnet became available, we have only the superconducting-state absorptivity data shown in Fig. 4. For the transition-metal films V-I, Ta-I, and Nb-I, which had upper critical fields in excess of those which could be provided by our magnet, we can also exhibit only A_S. However, calculations to be described in Sec. V lead us to believe that the latter three samples could be well characterized as being in the classical skin-effect

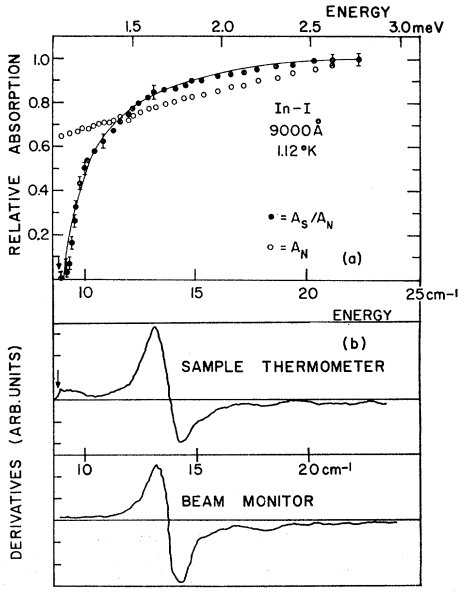

FIG. 9. (a) A_N and A_S/A_N for an In sample; (b) derivative signals.

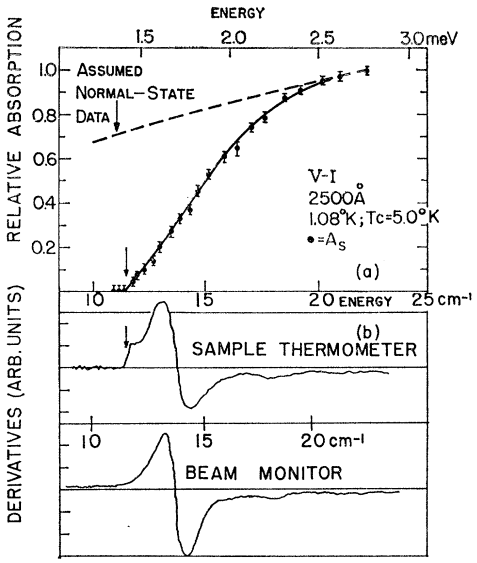

FIG. 10. (a) Superconducting-state absorptivity A_S for V sample, along with the assumed normal-state absorptivities used to obtain the edge shapes discussed in Sec. V-C; (b) derivative signals.

regime, where the surface resistance (and hence the absorptivity[34]) of a normal metal varies as $\omega^{1/2}$, where ω is the angular frequency of the radiation.[35] An assumed normal-state absorptivity of this form has therefore

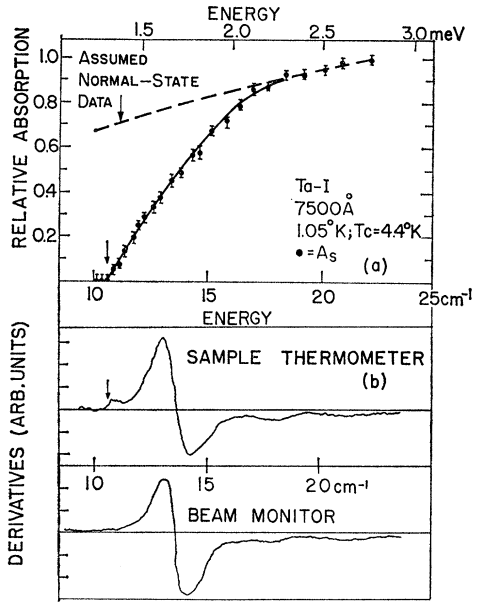

FIG. 11. (a) A_S and the assumed A_N for a Ta sample; (b) derivative signals.

[34] The expression for the absorptivity of bulk metal, which is valid for our thick films, is

$$A=4RZ_0/(Z^2+2RZ_0+Z_0^2)\cong 4R/Z_0,$$

where Z_0 is the impedance of free space, Z is the surface impedance of the metal, and $R=\mathrm{Re}(Z)$ is the metal's surface resistance. See. e.g., M. A. Biondi *et al.*, Rev. Mod. Phys. **30**, 1109 (1958),

[35] A. B. Pippard, in *Advances in Electronics and Electron Physics*, edited by L. Marton (Academic Press Inc., New York, 1954), Vol. 6, p. 1.

been included in the data for these films, which we present in Figs. 10–12.

While we shall discuss the various absorption spectra in detail in Sec. V, it is appropriate at this point to note a few of the more prominent feature of these curves. Our three Pb samples showed no evidence of the precursor absorption which had been previously reported by Ginsberg and Tinkham,[4] Richards and Tinkham,[6] Ginsberg and Leslie,[7] and by ourselves in an early report on our work with foil samples.[12] As we have described in detail elsewhere,[15] we believe that our previous observations were in error because of the presence of spurious high-energy radiation in the monochromator beam. This radiation was diffracted from the main grating in second order and reached the sample because of a faulty arrangement of the filters

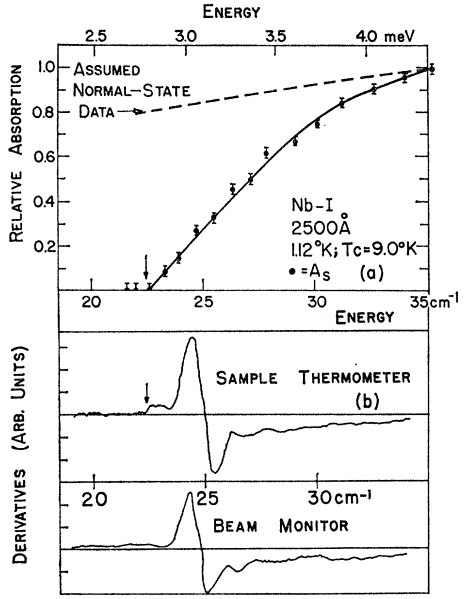

FIG. 12. (a) A_S and the assumed A_N for a Nb sample; (b) derivative signals.

within the monochromator. It is possible that a similar explanation could be given for the previous data of the other workers. In more recent transmission/reflection measurements on thin Pb films, Palmer[5] has reported the lack of a precursor; however, there was considerable scatter in his data and the existence of a 5% effect could not be precluded. Our data indicate that any precursor absorption in Pb must be less than 2% of the normal-state absorption at frequencies below the gap edge. The earlier work[4,6,7,12] reported the Pb precursor as a 10–20% effect. A similar effect was reported[4,6] in Hg; we were unable to check this because our apparatus was unsuitable for the preparation of Hg films.

We succeeded in observing structure indicative of multiple energy gaps in samples Pb-I, Pb-II, and Sn-I. In the case of the latter two samples, the structure was

sufficiently prominent to be seen in the absorption curves, even without the supporting evidence provided by the derivative data; see Figs. 6 and 8. For sample Pb-I the direct absorption curve was only slightly suggestive of structure, and it became necessary to examine the derivative data in more detail. In Fig. 5 we present a recorder tracing of the gap-region derivative-mode signals from the beam monitor and sample thermometer for this film. We can see from this figure that Pb-I had two absorption thresholds, at approximately 20.8 and 22.2 cm^{-1}. The threshold energy was taken to be that of the midpoint of the steps in the derivative curves. The smaller structure was not reproducible, and is not thought to have been significant.

In Table III we have summarized our findings for the energy gaps of our samples. The gap values are given in cm^{-1}, meV, and kT_c units to facilitate comparison with other experiments (Refs. 4, 6, 13, 31, 36–47, and 61). The details of such comparisons will be discussed in Sec. V. The experimental uncertainties quoted for our results represent the maximum variations observed in comparing several successive sweeps on each sample; we have included in Table III any uncertainties quoted by previous experimenters in discussing their work, as well as the numbers of samples examined by them in obtaining their results (where available).

V. DISCUSSION OF RESULTS

A. Electrodynamic Parameters

Before discussing the results obtained for our samples, it is useful to recall the roles played by certain combinations of parameters in determining the response of a metal to an oscillatory electromagnetic field.[35] The parameters involved are:

ω, the frequency of the radiation field;
τ, the mean time between collisions for an electron;
l, the mean free path of an electron;
δ, the classical electromagnetic skin depth;
ξ, the Pippard coherence length for superconductive electrodynamics;
λ, the electromagnetic penetration depth for a superconductor.

The salient facts concerning these parameters are these:

(1) If $\omega\tau \gtrsim 1$, inertial effects begin to manifest themselves. The conduction electrons are unable to follow the fields, and the frequency dependence of the surface resistance of the metal is reduced.

(2) If $l/\delta \gtrsim 1$, a nonsuperconducting metal begins to exhibit nonlocal behavior,[48] the current at a given point being governed by an integral of the electric field over a surrounding volume. In the extreme anomalous limit were $l/\delta \gg 1$, the surface resistance varies as $\omega^{2/3}$, rather than as $\omega^{1/2}$ as in the classical regime.

(3) For a superconductor, ξ/λ plays the same role in determining the applicability of local or nonlocal electrodynamics as does l/δ for a normal metal; if $\xi/\lambda \gtrsim 1$, nonlocal effects appear.

(4) The ratio l/ξ_0 determines the observability of anisotropy of the energy gap. Anderson[49] has shown that if $l/\xi_0 \gtrsim 1.6$, any anisotropy in the energy gap should be observable; the superconductor is said to be in the clean limit. In the dirty limit where $l/\xi_0 \ll 1.6$, scattering between all portions of the Fermi surface washes out the anisotropy, and only a single gap is observable.

These combinations of parameters have been evaluated for our samples and are tabulated in Table IV, with ω taken to be ω_g, the frequency of the radiation at the gap edge. The procedure employed to evaluate the parameters was the following:

(1) Measurements of the resistances of the monitor films (see Sec. III) at room temperature and at 4.2°K (or 9.2°K in the case of the Nb) gave the film resistivity ρ_F.

(2) For Pb, Sn, and In, attempts to calculate l_F (the mean free path in the film) by means of the ρl products tabulated by Chambers[50] (for Pb and Sn) and Toxen and Burns[51] (for In) generally resulted in values at 4.2°K in excess of the film thicknesses d; for these samples we set $l_F = d$. For V, Ta, and Nb, we take $l_F = 10^{-6}$ cm; this is a reasonable figure for the grain size in films of these metals, as found by Hauser and Theuerer.[52,53]

(3) The products $\omega_g\tau = \omega_g l_F/v_0$ (v_0 is the Fermi velocity) were evaluated using $v_0 = 0.50\times10^8$, 0.65×10^8, and 0.3×10^8 cm/sec for Pb,[54] Sn,[54] and Nb,[55] respectively, and $v_0 = 10^8$ cm/sec for In, V, and Ta.

[36] P. Townsend and J. Sutton, Phys. Rev. **128**, 591 (1962).
[37] N. V. Zavaritskii, Zh. Eksperim. i Teor. Fiz. **45**, 1839 (1963) [English transl.: Soviet Physics—JETP **18**, 1260 (1964)].
[38] J. G. Adler and J. S. Rogers, Phys. Rev. Letters **10**, 217 (1963).
[39] H. R. O'Neal and N. E. Phillips, Phys. Rev. **137**, A748 (1965).
[40] K. Fossheim and J. R. Leibowitz, Phys. Letters **22**, 140 (1966).
[41] V. D. Fil *et al.*, Zh. Eksperim. i Teor. Fiz. **52**, 891 (1967). [English transl.: Soviet Phys.—JETP **25**, 587 (1967)].
[42] R. Radebaugh and P. H. Keesom, Phys. Rev. **149**, 209 (1966); **149**, 217 (1966).
[43] H. V. Bohm and B. H. Horwitz, in *Proceeding of the Eighth International Conference on Low-Temperature Physics* (Butterworth and Company, Ltd., London, 1963), p. 191.
[44] I. Dietrich, in Ref. 43 above, p. 173.
[45] E. R. Dobbs and J. M. Perz, Rev. Mod. Phys. **36**, 257 (1964).
[46] R. Weber, Phys. Rev. **133**, A1487 (1964).
[47] L. Y. L. Shen *et al.*, Phys. Rev. Letters **14**, 1025 (1965).
[48] A stricter condition for the appearance of nonlocal effects is $(l/\delta) > (1+\omega^2\tau^2)^{3/4}$. See M. A. Biondi *et al.*, Phys. Rev. **136**, A1471 (1964).
[49] P. W. Anderson, J. Phys. Chem. Solids **11**, 26 (1959).
[50] R. G. Chambers, Proc. Roy. Soc. (London) **A215**, 481 (1952).
[51] A. M. Toxen and M. J. Burns, Phys. Rev. **130**, 1808 (1963).
[52] J. J. Hauser and H. C. Theuerer, Rev. Mod. Phys. **36**, 80 (1964).
[53] J. J. Hauser and H. C. Theuerer, Phys. Rev. **134**, A198 (1964).
[54] J. Bardeen and J. R. Schrieffer, in *Progress in Low-Temperature Physics*, edited by C. J. Gorter (North-Holland Publishing Co., Amsterdam, 1961), Vol. 3, p. 170.
[55] D. K. Finnemore *et al.*, Phys. Rev. **149**, 231 (1966).

TABLE III. Energy gaps observed.

Sample	This work cm^{-1}	This work meV	This work $2\Delta/kT_c$	Others (for the same material) meV	Others (for the same material) $2\Delta/kT_c$	Others (for the same material) Method[a]	Others (for the same material) N[b]	Ref.
Pb-I (Gap 1)	20.8±0.2	2.58±0.02	4.18±0.04		4.1±0.2	A	1	6
(Gap 2)	22.2±0.2	2.74±0.02	4.46±0.04	2.68	4.36	A	•••	61
Pb-II (Gap 1)	21.3±0.1	2.64±0.01	4.28±0.02		4.0±0.5	B	2	4
(Gap 2)	23.1±0.1	2.86±0.01	4.65±0.02	2.44±0.02		C	•••	13
Pb-III	21.5±0.1	2.67±0.01	4.34±0.02	2.52±0.02				
				2.97±0.02				
				2.67±0.05		C	•••	36
				2.90±0.05				
Sn-I (Gap 1)	9.30±0.1	1.15±0.01	3.58±0.04		3.6±0.2	A	1	6
(Gap 2)	9.85±0.2	1.24±0.02	3.86±0.08					
				1.10	3.42	A	•••	61
					3.3±0.2	B	2	4
				1.15±0.06		C	•••	36
				1.04−1.25		C	>100	37
In-I	8.7±0.1	1.08±0.01	3.69±0.04		4.1±0.2	A	1	6
					3.9±0.2	B	1	4
				1.10		C	•••	38
					3.26−3.77	D	1	39
					3.2±0.2[100], [011]	E	•••	40
					3.1±0.2[110]			
					3.45±0.1[100], [111]	E	•••	41
					3.35±0.1[110]			
					3.15±0.1[001]			
V-I	11.5±0.1	1.44±0.01	3.4±0.1		3.4±0.2	A	1	6
				1.45±0.10		C	1	31
					3.52±0.02	D	1	42
					3.20			
					0.10			
					3.1±0.2[100]	E	1	43
					3.2±0.2[111]			
					3.4±0.2[110]			
Ta-I	10.6±0.2	1.32±0.02	3.5±0.2		≤3	A	1	6
				1.30±0.05		C	1	31
				1.40±0.05	3.60±0.10	C	•••	36
					3.60±0.1[110]	C	1	44
					3.65±0.1[210]			
					3.65±0.1[211]			
					3.75±0.1[100]			
Nb-I	22.4±0.2	2.78±0.02	3.6±0.2		2.8±0.3	A	1	6
				2.90±0.05		C	1	31
				3.05±0.05		C	•••	36
					3.52	D	2	47
					0.32			
					3.63±0.06	E	•••	46
					3.77±0.03[100]	E	1	45
					3.74±0.04[111]			
					3.68±0.04[110]			

[a] Key: A, far-infrared absorption; B, far-infrared transmission; C, electron tunneling; D, specific heat; E, ultrasonic attenuation.
[b] Number of samples used.

(4) The classical skin depth δ was computed using $\delta=c/(2\pi\omega_0\sigma)^{1/2}$, where $\sigma=1/\rho_F$.

(5) The superconducting coherence length and penetration depth were evaluated using Tinkham's formula[56]

$$\xi^{-1}=\xi_0^{-1}+l_F^{-1}$$

and the relation[57]

$$\lambda=\lambda_0(1-t^4)^{-1/2}(1+\xi_0/l_F)^{1/2},$$

where $t=T/T_c$. The values of the bulk parameters ξ_0 and λ_0 were taken from the references listed in Table V.[58,59]

B. Discussion of Individual Samples

Having evaluated the electrodynamic parameters, we are now in a position to discuss the absorption spectra of the various samples in detail, and to compare our values for the energy gaps with those obtained by previous workers.

[56] M. Tinkham, Phys. Rev. **110**, 26 (1958).
[57] R. Meservey and D. H. Douglass, Jr., Phys. Rev. **135**, A24 (1964).
[58] J. M. Lock, Proc. Roy. Soc. (London) **A208**, 391 (1951).
[59] S. L. Wipf, Rev. Mod. Phys. **36**, 83 (1964).

In Fig. 4, as we have mentioned, we have the superconducting-state absorptivity for sample Pb-I. An examination of Table IV reveals that nonlocal effects should be beginning to come into play, with the frequency dependence being damped by inertial effects. The value of l/ξ_0 is sufficiently large so that the effects of anisotropy should be visible. As was discussed in Sec. IV, however, the use of the derivative data (Fig. 5) was required to make such effects visible. Because this sample had been kept at room temperature (under vacuum) for several days prior to the taking of the data in Fig. 4, it may be that sufficient annealing had taken place to provide one predominant crystallographic orientation; thus the absorptivity measurement would not probe all parts of the Fermi surface, and the data would be dominated by one energy gap.

The data on Pb-II and Pb-III are presented in Figs. 6 and 7. These data are more complete, the normal-state absorptivities being available. From Table IV, we see that Pb-II is further into the nonlocal regime, but is much more strongly affected by inertial effects; this presumably explains why the frequency dependences of the normal-state data for the two samples are not more different. On the other hand, Pb-II is in the clean limit (in the Anderson sense), while Pb-III has an l/ξ_0 ratio of only 1.4, which places it close to the dirty region. Indeed, the data show a well-resolved pair of gaps for Pb-II, but only a single gap for Pb-III. The Pb-II gaps agree very well with the values obtained by Townsend and Sutton[36] in their tunneling experiments, while the Pb-III gap lies slightly higher than the lower value for Pb-II. As Rochlin[13] has pointed out, values in the range 2.71–2.75 meV have been previously quoted for "the" Pb gap; our value of 2.67 meV for Pb-III would seem to agree with this range, while the 2.64 and 2.86 meV obtained for Pb-II straddle it. The figures of 2.58 and 2.75 meV for Pb-I are somewhat anomalous. The lower one agrees with one of Rochlin's "critical voltages" [13] which, however, has not been previously identified as arising from a single-energy gap (as opposed to being the sum of two half-gaps, which also gave rise to structure in Rochlin's tunneling data). The 2.75 meV figure is close to the upper end of the range of values associated with the "average" gap in Pb. It seems unlikely, however, that the annealing of this sample would have resulted in a predominantly "dirty" film, which is what would be required for the average gap to appear.

TABLE IV. Electrodynamic parameters of the samples.

Sample	$\omega_0\tau$	l/δ	ξ/λ	l/ξ_0
Pb-I	4.4	27	2.0	7.3
Pb-II	7.6	52	2.0	12
Pb-III	1.0	2.6	1.0	1.4
Sn-I	1.1	12.5	2.1	1.5
In-I	1.5	56	2.8	3.4
V-I	0.02	0.02	0.09	0.22
Ta-I	0.02	0.02	0.05	0.11
Nb-I	0.14	0.03	0.075	0.23

TABLE V. Bulk coherence lengths and penetration depths.

Material	ξ_0(Å)	Ref.	λ_0(Å)	Ref.
Pb	830	54	390	54
Sn	2300	54	510	54
In	2600	51	640	58
V	450	42	398	42
Ta	900	59	540	52
Nb	430	55	350	55

It should be noted that we have not identified any other structure in our absorption data as arising from the other critical energies reported by Rochlin. This lends support to the idea (put forth by him) that at least some of these values are not to be identified with distinct energy gaps, but are rather the result of averaging other gap values. Also, our gap values for Pb are higher than those reported by Richards and Tinkham[6] in their bulk-absorption work, and by Ginsberg and Tinkham[4] in their experiments on transmission through thin films. More recent far-infrared transmission and absorption measurements[5,60,61] give gap values of about 22 cm^{-1}, in agreement with our results.

Figures 8 and 9 contain the absorptivity ratios for Sn-I and In-I. Table IV reveals that both are in the anomalous skin-effect regime, with inertial effects just beginning to become important. Sn-I has about the same l/ξ_0 ratio as Pb-III, but does show evidence of two gaps. The lower of these agrees with the single value found by Townsend and Sutton,[36] while both of our values fall within the range reported by Zavaritskii[37] in his experiments involving tunneling into a single-crystal sample. It appears from our data that an l/ξ_0 ratio of 1.5 is near the minimum required for observation of multiple gaps in Sn employing our techniques. Our values for the Sn gaps are in somewhat better agreement with the earlier data of Tinkham and collaborators[4,6] than was the case for Pb; additional experiments by Richards[14] on far-infrared absorption in bulk single-crystal samples of Sn gave gap values which appear somewhat smaller, although no numerical values are assigned in his paper.

Drew and Sievers[61] have recently reported absorptivity studies on a Sn-foil light pipe which reveal a gap at 8.8 cm^{-1}, in fair agreement with our results.

Despite an l/ξ_0 ratio of 3.4, sample In-I failed to show gap anisotropy. Previous experiments have presented conflicting results concerning such anistropy in In; ultrasonic attenuation measurements by Fossheim and Leibowitz[40] revealed an anisotropy of at most 3%, while similar measurements by Fil *et al.*[41] revealed a

[60] W. S. Martin, Ph.D. thesis, University of California, Berkeley, 1965 (unpublished); and W. S. Martin and M. Tinkham, Phys. Rev. (to be published).

[61] H. D. Drew and A. J. Sievers, Bull. Am. Phys. Soc. **12**, 77 (1967).

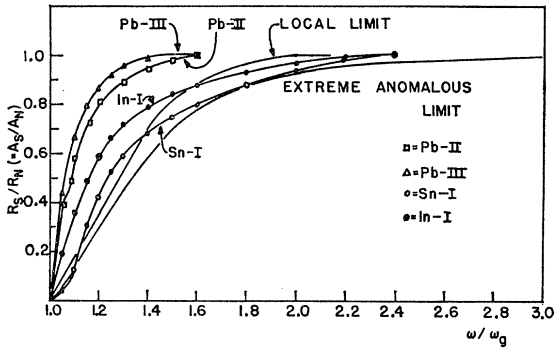

FIG. 13. Absorption edges A_S/A_N of samples Pb-II, Pb-III, Sn-I, and In-I, plotted against frequency normalized to the gap edge (the lower gap edge, in the case of Pb-II and Sn-I). The curve labeled "extreme anomalous limit" is the result of the theory of Mattis and Bardeen [Eq. (7)].

variation of almost 10%. The specific-heat data of O'Neal and Phillips,[39] (see Table III) give gap values of 3.26–3.77 kT_c, and can be well fitted by any *single* value within this range; the limiting values merely represent the extremes in the possible interpretation of the lattice contribution. Finally, it should be noted that the lack of anisotropy in our absorption data may merely reflect a strong orientation of the film; Toxen and Burns[51] have reported finding a very strong (101) orientation in In films. Our value of 8.7 cm^{-1} for the In gap is in good agreement with the earlier tunneling result of Adler and Rogers, and is somewhat lower than that found in the earlier far-infrared work.[4,6]

The superconducting-state data for V, Ta, and Nb are shown in Figs. 10–12. Table IV shows that all three of these samples were in the local limit, with no important inertial effects in evidence; for this reason, we have assumed that the normal-state absorptivity could be well represented by an $\omega^{1/2}$ dependence, and have included a curve of that form in the data. This assumption was necessary because our magnet was incapable of providing fields sufficient to drive these samples normal. (We performed the residual-resistance ratio measurements in another cryostat and with another magnet, which was capable of driving V-I and Ta-I normal. This latter equipment was not adaptable to the geometry of the far-infrared experiment.) The l/ξ_0 ratios for all three samples were too low to permit the observation of gap anisotropy. Such anisotropy has apparently been seen in V by Radebaugh and Keesom,[42] whose sample had a residual-resistance ratio an order of magnitude higher than that of our starting material (140 versus 14.4). Even this is somewhat surprising, as Garland[62] has predicted that *s-d* scattering should wash out gap anisotropy in transition metal samples of resistance ratio $\lesssim 10^4$. Dietrich[44] and Dobbs and Perz[45] have performed tunneling and ultrasonic attenuation experiments on Ta and Nb, respectively, and have found anisotropy which is only narrowly outside of experimental error. It is of interest to note that the specific-heat measurements on both V [42] and Nb [47] have indicated the presence of very small additional energy gaps, approximately one order of magnitude smaller than those usually measured. Shen *et al.*[47] have also reported such behavior for Ta and V, but without giving quantitative results for the gap values.

Our value of the gap in V is in good agreement with the values previously found in tunneling,[31] specific heat,[42] ultrasonic attenuation,[43] and bulk far-infrared[6] experiments. For Ta and Nb, we obtain values which are considerably larger than those found in the earlier bulk infrared work,[6] but in good agreement with more recent tunneling[31,36] and ultrasonic attenuation[45,46] results. This may merely reflect the advantage in terms of surface quality which our films held over the machined cavities used in the bulk-absorption measurements.

C. Comparison of the Absorption Edges with Theory

In Figs. 13 and 14 we have plotted the absorption edges of all of our samples, with the exception of Pb-I, versus a normalized frequency ω/ω_g, where ω_g is the frequency at the gap edge (the lower gap edge, in the case of multiple-gap samples Pb-II and Sn-I). In this way, we can compare our results with the predictions of the microscopic theory. The most familiar of such predictions are those of Mattis and Bardeen,[2] who treated the anomalous skin effect in superconductors and normal metals, and derived exrpessions for the ratios of theconductivities for the two states. If we denote by σ_N the conductivity of the normal state, and if the conductivity of the superconducting state is written as[13]

$$\sigma_S(\omega)=\sigma_1(\omega)-i\sigma_2(\omega), \tag{3}$$

then the Mattis-Bardeen results for zero temperature

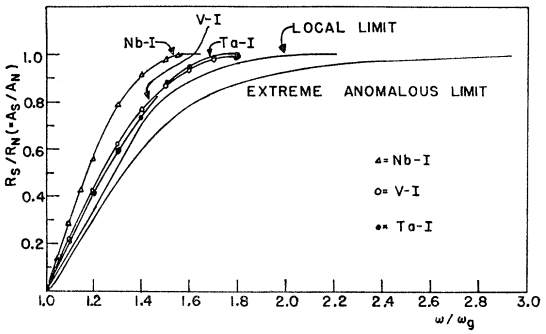

FIG. 14. Absorption edges of samples Ta-I, V-I, and Nb-I, compared with the Mattis-Bardeen result.

[62] J. W. Garland, Phys. Rev. Letters **11**, 111 (1963).

are

$$\frac{\sigma_1(\omega)}{\sigma_N}=\left(1+\frac{\omega_g}{\omega}\right)E(k)-2\left(\frac{\omega_g}{\omega}\right)K(k), \qquad \omega>\omega_g$$

$$\frac{\sigma_2(\omega)}{\sigma_N}=\frac{1}{2}\left[\left(\frac{\omega_g}{\omega}+1\right)E(k')+\left(\frac{\omega_g}{\omega}-1\right)K(k')\right]. \quad (4)$$

Here E and K are elliptic integrals of the indicated arguments;

$$k=|\,1-\omega/\omega_g\,|/|\,1+\omega/\omega_g\,|; \qquad k'=(1-k^2)^{1/2}. \quad (5)$$

As Tinkham[63] has pointed out, we can now compute the theoretical ratio of absorptivity in the superconducting and normal states using the further Mattis-Bardeen relation for surface impedances

$$Z_{S\infty}/Z_{N\infty}=\{[\sigma_1(\omega)-i\sigma_2(\omega)]/\sigma_N\}^{-1/3}$$

and

$$Z_{N\infty}=(1+i\sqrt{3})\,R_{N\infty} \quad (6)$$

to obtain the surface-resistance ratio

$$\frac{R_{S\infty}}{R_{N\infty}}=\frac{2\sin\frac{1}{3}\theta}{[(\sigma_1(\omega)/\sigma_N)^2+(\sigma_2(\omega)/\sigma_N)^2]^{1/6}}, \quad (7)$$

where

$$\theta=\tan^{-1}(\sigma_1(\omega)/\sigma_2(\omega)).$$

This ratio has been plotted as the "extreme anomalous limit" in Figs. 13 and 14.

As can be seen from Table IV, none of our samples was really in the extreme anomalous limit in the superconducting state; In-I, with $\xi/\lambda=2.8$, came the closest. Therefore, it is not surprising that there is not better agreement between the Mattis-Bardeen curve and our results. We find, as have previous workers,[6,7] that our absorption edges are considerably steeper than the theoretical prediction, which is[63]

$$\left.\frac{d(R_{S\infty}/R_{N\infty})}{d(\omega/\omega_g)}\right|_{\omega=\omega_g}=\tfrac{1}{3}\pi. \quad (8)$$

Our values for this slope range from $\sim$1, in the case of Sn-I, to $\sim$8.5 for Pb-III. The Sn-I curve appears to be in better agreement with the theory at low energies due to the shape imparted to the experimental curve by the smaller energy gap.

Tinkham[63] has discussed this common discrepancy, and has argued that much of it arises from the fact that it is quite possible to prepare samples for which $l\gg\delta$, so that the metal is in the extreme anomalous limit when driven into the normal state, while $\xi/\lambda\sim1$, meaning that this limit of the theory is not correct for the superconducting state. This was indeed the case for our samples Pb-II, Sn-I, and In-I, as can be seen from Table IV.

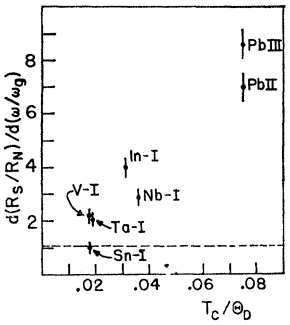

FIG. 15. The initial slopes of the various normalized absorption edges, $d(R_s/R_N)/d(\omega/\omega_g)$, plotted versus the ratio of transition temperature to Debye temperature. The Mattis–Bardeen theory predicts an initial slope of $\frac{1}{3}\pi$, which is shown by the dashed line.

The other case commonly discussed is that of the local limit, in which $\delta\gg l$ for a normal metal, or $\lambda\gg\xi$ for a superconductor. In this case, we have for the surface impedance ratio[6]

$$Z_S/Z_N=\{[\sigma_1(\omega)-i\sigma_2(\omega)]/\sigma_N\}^{-1/2},$$
$$Z_N=(1+i)\,R_N, \quad (9)$$

and for the surface-resistance ratio

$$\frac{R_S}{R_N}=\frac{\sqrt{2}\sin\frac{1}{2}\theta}{[(\sigma_1(\omega)/\sigma_N)^2+(\sigma_2(\omega)/\sigma_N)^2]^{1/4}}, \quad (10)$$
$$\theta=\tan^{-1}(\sigma_1(\omega)/\sigma_2(\omega)).$$

The initial slope is now $\pi/2^{3/2}$. The corresponding curve is also plotted in Figs. 13 and 14. It is a somewhat better approximation to the V and Ta data than is the extreme anomalous limit, but the fit to Pb, Sn, In, and Nb is not markedly improved. Recently, Ginsberg[64] has described a series of calculations for the shape of the absorption edge in Pb:Tl and Pb:Bi alloys, employing neither the extreme anomalous nor the extreme local limits. He has succeeded in obtaining theoretical results for these short mean-free-path metals which show considerable steepening of the edge as compared to the earlier theories. However, the experimentally observed edges remain steeper than the predictions.

In Fig. 15 we summarize our findings by plotting the initial slopes of the normalized absorption curves versus T_c/Θ_D, the ratio of the transition temperature to the Debye temperature of the various metals. This quantity provides a measure of the strength of the electron-phonon interaction; the larger its value, the more the superconductor would be expected to deviate from the simple BCS behavior. We see that this is generally the case insofar as the normalized slope tends to be an increasing function of T_c/Θ_D. Such a variation is to be

[63] M. Tinkham, in *Optical Properties and Electronic Structure of Metals and Alloys*, edited by F. Abeles (North-Holland Publishing Co., Amsterdam, 1966), p. 431.

[64] D. M. Ginsberg, Phys. Rev. **151**, 241 (1966).

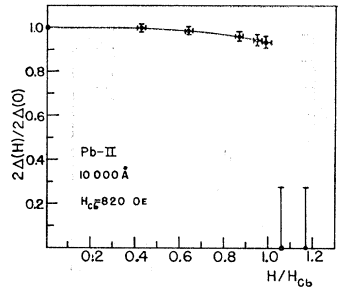

FIG. 16. Magnetic field dependence of the lower energy gap for sample Pb-II. H_{cb} is the bulk critical field. The superconducting surface sheath is apparently gapless; the large error flags on the two highest-field points indicate our inability to carry our investigations to zero energy.

expected, for $T_c \sim \lambda/\xi_0$ and as Tinkham[63] has pointed out, the ratio R_S/R_N near ω_g will differ from (7) by an amount which increases with λ/ξ_0. In addition, Palmer and Tinkham[5] have shown that strong electron-phonon coupling of the sort considered by Nam[65] leads to deviations from the Mattis-Bardeen conductivities which are of such a sign as to lead directly to a steepening of the absorption edge.

D. Magnetic Field Dependence of the Energy Gap in Pb

In the course of these experiments, we measured the position of the first (i.e., lower-energy) absorption edge in sample Pb-II as a function of magnetic field. This represents the first observation by calorimetric techniques of the apparent gap value at various field strengths. The Ginzburg-Landau[66] theory predicts that a film of thickness $d<(\sqrt{5})\lambda$ will undergo a second-order phase transition at the critical field, the order parameter (which is proportional to the energy gap if the latter does not vary too rapidly in space) decreasing continuously to zero; on the other hand, a thick film will show a discontinuous drop in the gap value, i.e., a first-order transition. Our film Pb-II, with $d/\lambda \approx 26$, is clearly in this second category. In Fig. 16 we have our results for the lower energy gap expressed as a fraction of its zero-field value (21.4 cm^{-1}), plotted versus H/H_{cb}, where $H_{cb}=820$ Oe is the critical field for bulk Pb. The discontinuous drop in the gap 2Δ is indeed observed; while our monochromator was not capable of generating useful amounts of radiation much below 6 cm^{-1} $[0.28\times 2\Delta(0)]$, we believe that the absence of a gap larger than that energy is indicative of its complete vanishing.

The absence of a gap in the excitation spectrum above H_{cb} is interesting in light of the demonstration by Saint-James and de Gennes[67] that films of certain metals, including pure Pb, can support a superconducting surface sheath when magnetic fields in excess of H_{cb} are applied parallel to the film plane. Such a sheath, approximately one coherence length thick, can persist up to a field

$$H_{c3}=\sqrt{2}C\kappa H_{cb} \qquad (11)$$

where κ is the Ginzburg-Landau[66] parameter and C is a constant equal to 1.69. Thus if $\sqrt{2}C\kappa>1$, the effects of the sheath should be observable above H_{cb}. The temperature dependence found by Paskin *et al.*[68] leads to the value $\kappa(\mathrm{Pb})=0.54$ at 1.10°K, the temperature of our measurements. Hence $\sqrt{2}C\kappa=1.29$, and the sheath should be observable up to $H_{c3}=1060$ Oe.

Rosenblum and Cardona[69] have obtained evidence for such a sheath in dilute Pb:Tl alloys and pure Pb by means of a microwave surface-impedance technique, and Goldstein[70] and Burger *et al.*[71] have seen its effects in tunneling experiments. These results are not inconsistent with a gapless excitation spectrum; in fact, the rapid drop in the conductance peak observed by Goldstein above H_{cb} is very suggestive of the filling-in of the energy gap by a continuum of states. This picture is also consistent with the millimeter-wave absorption measurements of White and Tinkham,[72] and in fact they suggested the possibility of the vanishing of the gap. They also pointed out that it may not be sufficient to describe the effect of a magnetic field on a superconductor by simply assigning a field-dependence to the gap parameter.

In any event, the data presented in Fig. 16 show a drop of approximately 7% in the value of the lower energy gap from $H=0$ to $H=H_{cb}$ (the upper gap followed a similar curve, but became indistinct near H_{cb}); this is typical of the magnitude of gap variation found by Morris and Tinkham[33] for a thick In film. The theoretical result of Ginzburg and Landau[66] for a superconducting half-space (e.g., a thick film) with H parallel to the surface is

$$\psi(x, H)/\psi_0=1-D(x)\,(H/H_{cb})^2,$$
$$D(x)=[\kappa/(2-\kappa^2)\sqrt{8}]$$
$$\times\{\exp(-\sqrt{2}\kappa x/\lambda_L)-\tfrac{1}{2}\kappa\exp(-2x/\lambda_L)\}, \qquad (12)$$

where x is the distance below the surface of the metal, λ_L is the London penetration depth,[73] and the order parameter ψ is proportional to the energy gap (ψ_0 is the value of ψ in the absence of the field). Evaluating these expressions at the surface ($x=0$), we obtain for Pb

$$\psi(0, H)/\psi_0=1-0.081(H/H_{cb})^2,$$

[65] S. B. Nam, Phys. Rev. **156**, 470, 487 (1967).
[66] V. L. Ginzburg and L. D. Landau, Zh. Eksperim. i Teor. Fiz. **20**, 1064 (1950).
[67] D. Saint-James and P. G. de Gennes, Phys. Letters **7**, 306 (1963).
[68] A. Paskin *et al.*, Phys. Rev. **137**, A1816 (1965).
[69] B. Rosenblum and M. Cardona, Phys. Letters **9**, 220 (1964).
[70] Y. Goldstein, in *Proceedings of the Ninth International Conference on Low-Temperature Physics*, edited by J. G. Daunt *et al.* (Plenum Press, New York, 1965), Vol. A, p. 400.
[71] J. P. Burger *et al.*, Phys. Rev. **137**, A853 (1965).
[72] R. H. White and M. Tinkham, Phys. Rev. **136**, A203 (1964).
[73] F. London, *Superfluids* (Dover Publications, Inc., New York, 1961), Vol. 1, p. 33.

or an 8.1% decrease in the gap at H_{cb}. If, however, Eqs. (12) are averaged over the superconducting half-space, weighted with a factor $\exp(-2x/\lambda_L)$ to represent the penetration of an electromagnetic field, the decrease at H_{cb} is 6.6%. Our value of 7% is thus in fair agreement with these predictions. It would perhaps be unwise to expect more exact agreement on this point; the applied field cannot be made exactly parallel to the sample film at all points, and the perpendicular component will result in flux penetration in the form of quantized vortices.[60] Such vortices are characterized by position-dependent order parameters, so that it can become quite difficult to characterize the entire sample by a single gap value; we then no longer have the clean situation to which the theory pertains.

ACKNOWLEDGMENTS

It is a pleasure to thank Dr. D. H. Douglass, Jr., who originally suggested this problem, for his advice and encouragement throughout the course of the experiment. I would also like to thank Professor M H. Cohen and Dr. M. Strongin for helpful discussions on several points. Dr. P. L. Richards and Dr. D. M. Ginsberg provided advice on various questions of far-infrared technique. I am also grateful to the Low-Temperature Laboratory (supported by the National Science Foundation) and the Materials Preparation Laboratory (supported by the Advanced Research Projects Agency) for the use of their facilities and the technical assistance of their personnel.

PHYSICAL REVIEW VOLUME 167, NUMBER 2 10 MARCH 1968

Boundary Condition on the Order Parameter at a Tunneling Barrier in a Pure Superconductor ($T=T_c$)

R. G. Boyd

Department of Physics and Astrophysics, University of Colorado, Boulder, Colorado

(Received 14 August 1967)

We consider the nucleation of superconductivity at a δ-function plane barrier in a free-electron superconductor. We calculate the exact kernel of Gorkov's linear integral equation for the order parameter Δ, and compare it with the kernel derived by de Gennes for a similar model on the basis of a correlation-function argument which has not been rigorously justified as yet. The two kernels are not the same, particularly near the barrier, but the difference oscillates with wavelength π/k_F and is negligible for the purpose of calculating asymptotic boundary conditions on the order parameter. We thus confirm for our model the boundary condition predicted by de Gennes, $\psi_+=\psi_-+(\langle 1-t\rangle/\langle t\rangle)\xi_0 d\psi/dx\,|_0$.

I. INTRODUCTION

In this paper, we study the functional form of the order parameter $\Delta(\mathbf{r})$ near a plane tunneling barrier in a pure superconductor.

We restrict our attention to the neighborhood of a second-order phase transition, where the order parameter $\Delta(r)$ obeys Gorkov's equation[1,2]

$$\Delta(\mathbf{r})=\int K(\mathbf{r},\mathbf{r}')\Delta(\mathbf{r}')d^3r'. \tag{1}$$

In particular, we assume $T=T_c$ and $H=0$. Gorkov's equation then has one-dimensional solutions $\Delta(x)$.

We represent the superconductor with the BCS free-electron model with pairing interaction of strength V. We represent the barrier with the repulsive δ-function potential $(\kappa/m)\delta(x)$. The electron wave functions ψ_n satisfy the Schrödinger equation[3]

$$[-(\nabla^2/2m)+(\kappa/m)\delta(x)]\psi_n=E_n\psi_n, \tag{2}$$

which can be solved exactly.

In Sec. II, we calculate the thermal Green's function[4]

$$G_\omega(\mathbf{r},\mathbf{r}')=\sum_n \psi_n(\mathbf{r})\psi_n^*(\mathbf{r}')/(i\omega-\epsilon_n) \tag{3}$$

from the exact wave functions. We then calculate the kernel of Gorkov's equation[5]

$$K(\mathbf{r},\mathbf{r}')=VT_c\sum_\omega G_\omega(\mathbf{r},\mathbf{r}')G_\omega^*(\mathbf{r}',\mathbf{r}). \tag{4}$$

We have not found an exact solution to Gorkov's equation. Instead, we proceed approximately by substituting zero-order solutions $\Delta_0(x)$ in Gorkov's

[1] L. P. Gorkov, Zh. Eksperim. i Teor. Fiz. **36**, 1918 (1959) [English transl.: Soviet Phys.—JETP **9**, 1364 (1959)].

[2] A. A. Abrikosov, L. P. Gorkov, and I. E. Dzyaloshinski, *Methods of Quantum Field Theory in Statistical Physics* (Prentice-Hall, Englewood Cliffs, N.J., 1963), Chap. 7.

[3] Natural units $\hbar=c=k_B=1$ are used throughout this paper.

[4] See Ref. 2, Chap. 3. Here $\epsilon_n=E_n-\mu$.

[5] See Ref. 2. The sum is over $\omega=2\pi T_c(n+\frac{1}{2})$ from $n=-\infty$ to $+\infty$.